

Chapter 33

Study of Shallow Soil Deposit in East Coast of India by SPT, MASW, and Crosshole Tests



Ayush Kumar, Anbazhagan Panjamani, Ravinesh Kumar, and K. R. Lenin

Introduction

Earthquakes cause various hazards such as landslides, liquefaction, ground shaking, flooding, and tsunamis. Among these, liquefaction has been known to cause the failure of even well-designed and well-built structures as it is entirely a property of the subsurface soil. Liquefaction is defined as the transformation of granular material from solid to a liquefied state because of increased pore water pressure and reduced effective stress under seismic or cyclic loads.

In-situ seismic testing methods are commonly used for subsurface seismic velocity profiling which assists in the determination of low-strain stiffness of geological materials. With time, there has been an increase in the need for critical infrastructure; hence, the need for such tests is also increasing for efficient engineering design. With time and experience, in-situ test results have been used to estimate soil resistance against seismic hazards such as liquefaction. In-situ tests help determine the soil properties in their natural, undisturbed state. These tests are easy to perform at the site and reduce the dependency on laboratory tests which are often time-consuming, expensive, and require specific monitoring of the specimen properties [24].

The objective of this survey was to obtain the distribution of soil materials and S-wave velocities (V_S) of the shallow subsurface for the computation of elastic engineering properties of the subsurface strata. Standard penetration test and seismic tests of Crosshole Seismic Test (CHT) and MASW test were performed. Hammer energy correction was assigned to the equipment based on energy measurements from past studies on the same and similar equipment [3]. The velocity profiles obtained from

A. Kumar · A. Panjamani (✉) · R. Kumar
Indian Institute of Science, Bangalore, Karnataka 560021, India
e-mail: anbazhagan@iisc.ac.in

K. R. Lenin
Seccon Pvt. Ltd, Bangalore, Karnataka, India

MASW were coherent with the borehole records showing the gradual increase in the velocity values from gravelly silty sand at the top to the weathered limestone zone at the bottom of boreholes. Velocity profiles obtained from CHT showed higher velocity values than those obtained from MASW. This difference could have been due to the highly localized and confined nature of Crosshole testing between the boreholes and dispersed, and broader (global) coverage in the MASW test, where velocities measured are averaged out over the travel path length. N -values and V_S values thus obtained were used to estimate factor of safety against liquefaction (FS_L) for subsurface silty sand layers submerged under shallow groundwater.

Site Location and Description

The investigation was carried out in the coastal city of Tuticorin, located along the Eastern coast of Tamil Nadu, India. The testing site is located about 1.5 km west of seashore near Southern Petrochemical Industries Corporation (SPIC) Township consisting of level to gently sloping ground. The project area is covered with the fluvial, fluvio-marine, Aeolian, and unconsolidated marine sediments of the quaternary age, which are underlain by medium to coarse-grained tertiary sandstone and claystone. The groundwater table is present at 1.65 m depth below ground level. The site is in seismic zone II as per the seismic zoning map of India in IS: 1893 (Part I)-2016, which is based on past intensity and not based on possible seismic hazard parameters in the region [2].

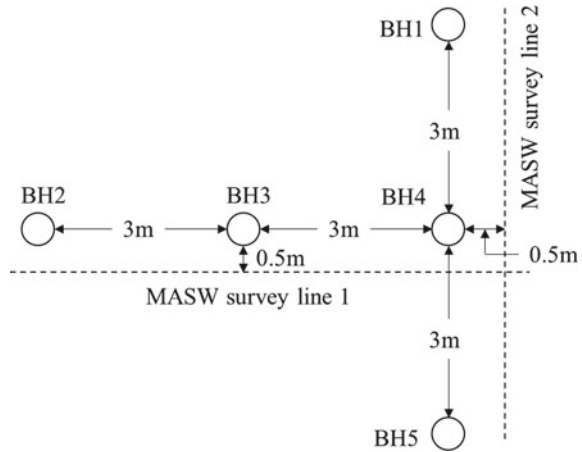
Investigation Methods

This study involved the use of multiple exploration methods like SPT, CHT, and MASW. There have been limited studies in the Indian region with multiple approaches to determine subsurface properties. Since each method determines V_S differently and has its own interpretation, using a single method for important analysis such as liquefaction evaluation may not give sufficient estimation accuracy. These different site characterization tools have complementary roles in most situations and are most effectively used in combinations [9]. A brief description of the tests used and the profiles generated is presented in the following subsections.

Standard Penetration Test

The standard penetration test (SPT) is an in-situ dynamic penetration test designed to provide information on the geotechnical engineering properties of soil. This test is the

Fig. 33.1 Layout of boreholes for crosshole tests and location of MASW survey lines



most commonly used subsurface exploration method due to its workability and cost-effectiveness. The test provides samples for identification purposes and measures penetration resistance, which can be used for geotechnical design purposes.

SPT is of great use in cases where it is difficult to obtain undisturbed samples for testing, such as gravelly, sandy, silty, sandy clay, or weak rock formations. It is often used to approximate the in-situ density and angle of shearing resistance of cohesion-less soils and the strength of cohesive soils. Several other dynamic and static properties of subsoil layers are well correlated with SPT results [1, 4, 5]. The SPT is most widely used for empirical determination of a sand layer's susceptibility to soil liquefaction in India and also other places.

Hammer energy measurement is an integral part of the SPT procedure. Most of the empirical relations of N-value with static or dynamic soil properties are defined for a specific energy value [10]. If standard or any random energy value is assumed instead of the in-situ measurement, it will lead to erroneous calculations. For the same equipment and operator, the hammer energy ratio (measured energy/theoretical energy) (ER) values were measured previously in the range of 30–40%. The same range is assigned to the equipment, and analysis for liquefaction estimation has been carried out considering three ER values 30, 35, and 40%. In the current study, five boreholes were drilled in a T-shaped geometry (Fig. 33.1). SPT was performed in BH4. The depth profile of N-values with depth is presented in Fig. 33.2a. The N-values at refusal were estimated by extrapolation.

Crosshole Test

Crosshole test involves the determination of the velocity of horizontally travelling P-wave and S-wave in subsurface soil and rock strata between two or more boreholes. This method provides inputs for static/dynamic analyses as a means for computing

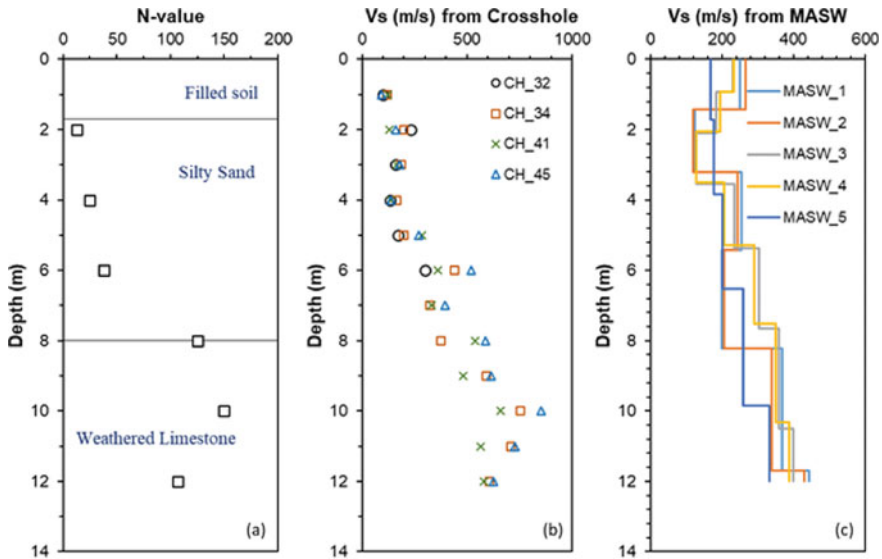


Fig. 33.2 a SPT N-values and V_S profiles at the site from b crosshole and c MASW tests

V_S , V_P , shear modulus, Young’s modulus, and Poisson’s ratio, or simply for the determination of anomalies that might exist between boreholes [22]. Typical test applications involve bridge/dam foundation analysis, in-situ materials testing, soil and rock mechanics, earthquake engineering, and liquefaction analysis.

Crosshole survey involves lowering a seismic source in one borehole and a 3 (or more) component geophone borehole receiver in the adjacent borehole(s) at the same depth, and impulses from the source are recorded in the receiver. The velocity of seismic waves is calculated by dividing distances between the boreholes by travel times of the recorded waveforms as per ASTM D4428-2000 and IS 13372-1992 part 2.

In the current study, CHT was conducted in four sets, denoted by CH₃₂, CH₃₄, CH₄₁, and CH₄₅, where CH_{ij} means the source is lowered in BH_i and the receiver in BH_j. Figure 33.3 shows the field setup for the Crosshole test. BIS-SH sparker source and BGK5 borehole receiver (Getomographie GmbH) and Geode seismograph (Geometrics, Inc.) are used for data acquisition. The V_S profiles obtained from CHT are given in Fig. 33.2b. Although the tests were conducted till 20 m depth, the profile is shown only up to 12 m because of the scope of analysis in this study.

MASW Test

The MASW survey is a seismic method used for evaluating the low-strain properties of the subsurface. It utilizes the dispersive nature of the surface waves to determine

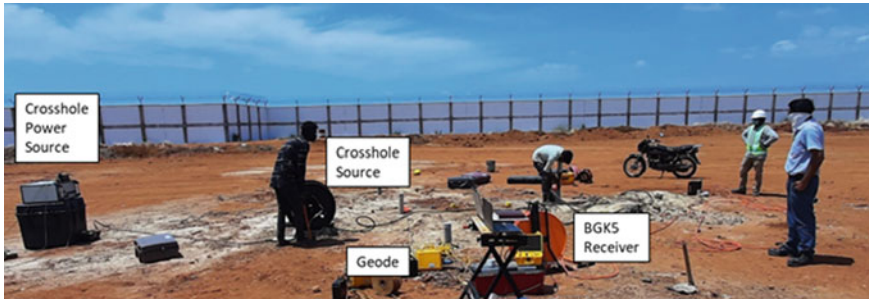


Fig. 33.3 Crosshole test setup in the field

the elastic properties of the half-space inverting the recorded field data [14, 15]. The MASW test has become a widely practised technique due to its use of multiple channels for data acquisition of surface waves. MASW technique offers high resolution and high signal-to-noise ratio. The Rayleigh waves offer the mode with the highest energy content among different waves produced during impact [23] and hence is used for the test. Post data acquisition and conventional signal processing techniques could be used for removing the ambient noise from the data and increase signal strength.

MASW system consisting of a 24-channel Geode seismograph with 24 numbers of vertical geophones of 4.5 Hz frequency has been used to carry out field experiments. MASW tests have been carried out with geophone intervals of 1 m. The source has been placed at 6 and 12 m from the nearest geophone to avoid the near-field and far-field effect [15]. The seismic waves are created by hitting a 17.6 lbs sledgehammer on a 300 mm × 300 mm metal plate with five stacks.

MASW tests were conducted near all five boreholes. Twenty-four geophones were used with 1 m receiver spacing and 10 m source distance from the nearest geophone. V_S profiles upto top 12 m of subsurface obtained from MASW test are presented in Fig. 33.2c. The seismic record for a typical MASW test is shown in Fig. 33.4. The phase velocity (V_ϕ)- frequency dispersion image and V_S profile from MASW for BH3, is shown in Fig. 33.5.

Evaluation of Liquefaction

In general, it is tedious to re-establish an in-situ stress state in the laboratory, and often soil specimens are too disturbed to yield relevant results. Sampling for undisturbed samples in granular soils requires specialized techniques, which are costly. Hence, field tests have become the state of practice for routine liquefaction investigations. Several methods have been developed to evaluate the safety of soil against liquefaction during a seismic event. Several field tests have been found to be helpful in evaluating liquefaction resistance, mainly SPT and V_S -based methods.

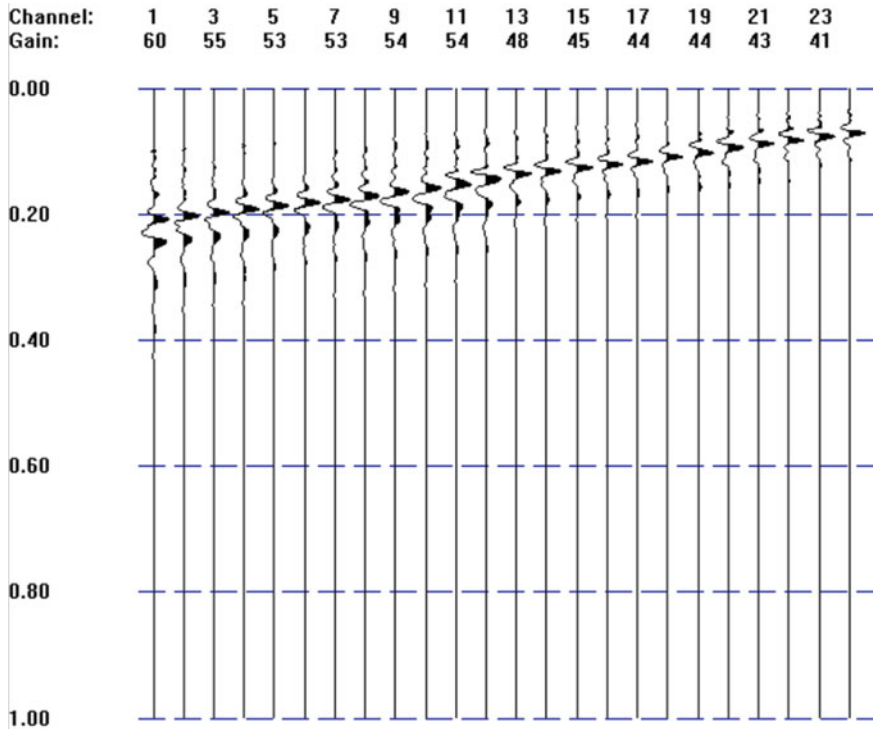


Fig. 33.4 Seismic record obtained from a typical MASW test at the site

Over the years, the ‘simplified procedure’ has evolved as the primary method for evaluating liquefaction resistance of soils. It was first developed by Seed and Idriss [18] as a stress-based approach and later improved by several researchers [6, 9, 16, 24] to enhance the applicability over various regions and improve the accuracy of soil behaviour prediction. For estimation of liquefaction resistance, two variables need to be calculated (1) seismic demand on the soil layer, also known as cyclic stress ratio (CSR) and (2) the capacity of the soil to resist liquefaction, known as cyclic resistance ratio (CRR). Evaluation of CSR is simple and needs the information of peak ground acceleration (0), total and effective stresses and depth of soil layers. The equation to calculate CSR [18] is given by

$$CSR = \left(\frac{\tau_{av}}{\sigma'_{v0}} \right) = 0.65 \frac{a_{max}}{g} \frac{\sigma_{v0}}{\sigma'_{v0}} r_d \tag{33.1}$$

where a_{max} = PHA at the ground surface due to earthquake, g = acceleration due to gravity, σ_{v0} = total vertical stress, σ'_{v0} = effective vertical stress, τ_{av} = effective shear stress (calculated for the effective number of loading cycles leading to liquefaction),

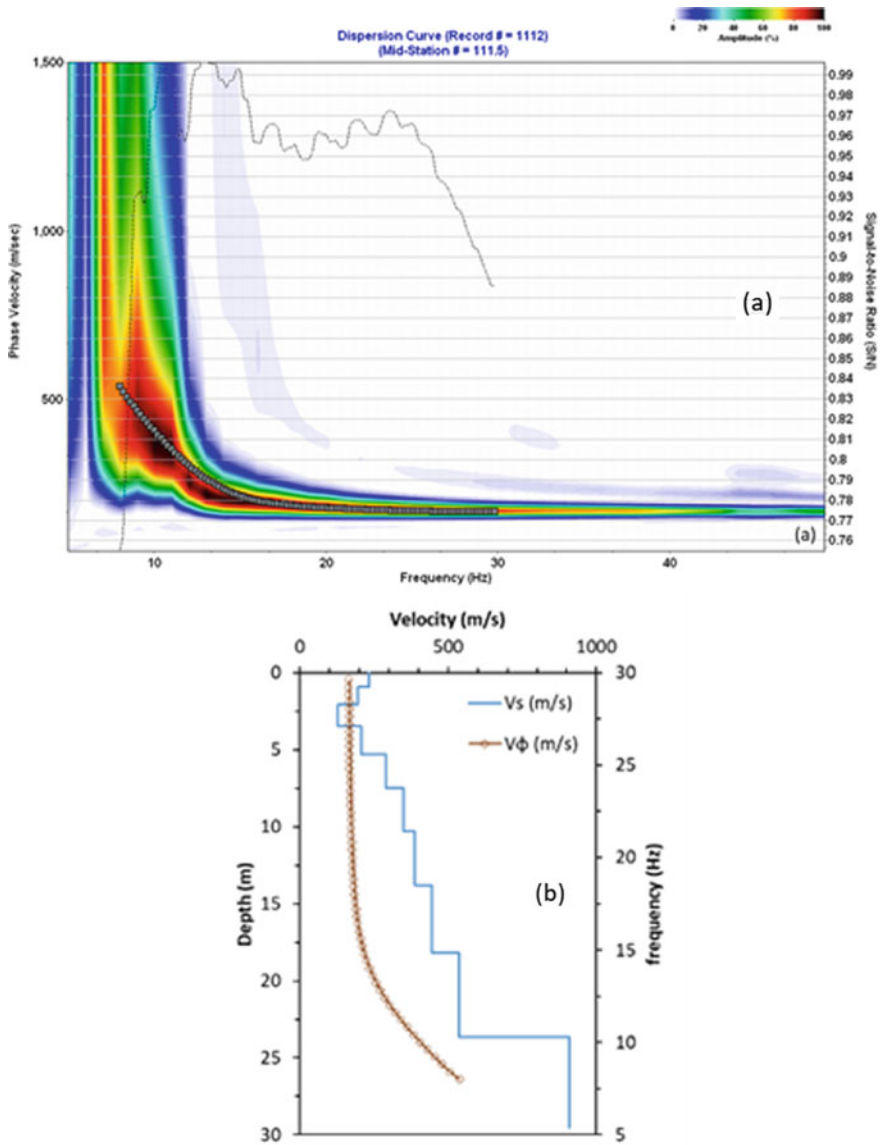


Fig. 33.5 a Dispersion image with dispersion curve and b 1D V_S profile with dispersion curve

r_d = stress reduction factor accounting for flexibility of soil with depth, estimated from Idriss [11].

For evaluation of CRR, two popular approaches are based on SPT and V_S .

SPT-Based Method

Liquefaction studies played an important role in standardizing the SPT procedure by improving SPT corrections such as overburden correction, energy correction, and fines content (FC) correction. In this method, the N-values are corrected for overburden, rod length, borehole diameter, sampler liner, hammer energy, and FC. The final corrected value is represented as $(N_1)_{60cs}$. The estimation of CRR is adjusted to the moment magnitude (M_w) of 7.5 ($CRR_{7.5}$). A magnitude scaling factor (MSF) is used to extend the usage to other magnitudes. Recent improvements in the calculation procedure are summarized in Boulanger and Idriss [9], and the same is followed in this study. Calculation of $CRR_{7.5}$ from $(N_1)_{60cs}$ is given by Boulanger and Idriss [9]:

$$CRR_{7.5} = \exp \left\{ \frac{(N_1)_{60cs}}{14.1} + \left(\frac{(N_1)_{60cs}}{126} \right)^2 - \left(\frac{(N_1)_{60cs}}{23.6} \right)^3 + \left(\frac{(N_1)_{60cs}}{25.4} \right)^4 - 2.8 \right\} \quad (33.2)$$

V_S-based Method

Small strain V_S has emerged as a promising alternative to penetration methods for liquefaction resistance evaluation. Based on the observation, both V_S and liquefaction resistance are similarly influenced by the same factors (e.g. void ratio, stress state and history, and geologic age). Some advantages of using V_S as a parameter are (1) easy in-situ measurement for hard-to-sample soils such as gravels and (2) direct relation to low-strain shear modulus G_{max} [7, 17, 20] (Andrus and Stokoe 1998), and easy procedure of MASW for V_S estimation. However, some concerns do exist regarding the use of V_S , which include (1) no sample collection, (2) possibility of undetected thin low V_S strata, and (3) confinement of method to the low-strain domain [7, 21].

This method relates overburden corrected V_S (V_{S1}) with CRR for different acceptable contents [7]. V_{S1} can be estimated using the relation

$$V_{s1} = V_s * \left(\frac{P_a}{\sigma'_v} \right)^{0.25} \quad (33.3)$$

Andrus and Stokoe [6] provided an upper limit V_{S1}^* to V_{S1} for cyclic liquefaction occurrence considering different case studies in China, Japan, Taiwan, and USA. V_{S1}^* can be calculated for different fine content, and CRR can be estimated if $V_{S1} \leq V_{S1}^*$. $CRR_{7.5}$ from V_{S1} can be calculated using the relation Andrus and Stokoe [7]

$$CRR = \left\{ a \left(\frac{V_{s1}}{100} \right)^2 + b \left(\frac{1}{V_{s1}^* - V_{s1}} - \frac{1}{V_{s1}^*} \right) \right\}$$

$$a = 0.0022, b = 2.8 \quad (33.4)$$

where

$$\begin{aligned} V_{s1}^* &= 215 \text{ m/s, for sands with FC} \leq 5\% \\ V_{s1}^* &= 215 - 0.5 * (\text{FC} - 5) \text{ m/s, for sands with } 5\% < \text{FC} < 35\% \\ V_{s1}^* &= 200 \text{ m/s, for sands and silts with FC} \geq 35\% \end{aligned} \quad (33.5)$$

Results and Discussion

The Factor of Safety Against Liquefaction

Using SPT N-value data

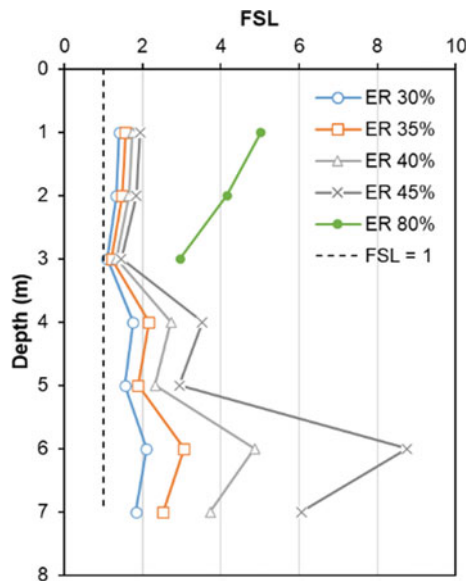
Table 33.1 gives a sample calculation for correction of measured N-values at 35% ER and estimation of $(N_1)_{60cs}$. Sampler correction and borehole diameter correction are considered as unity as per standard recommendations [10]. Hammer energy corrections were taken from previously available measurements on the same equipment and operator. ER was found to be in the range of 30–40%, which concurs with previous measurements in India by Selvam et al. (2020), Anbazhagan and Sagar [3], and Anbazhagan et al. [4]. Hence, three different energy corrections for 30, 35, and 40% ER were applied, and changes in FS_L values were studied. It is to be noted that the Indian code for earthquake resistance design IS 1893 (Part 1) [13] suggests single standard correction values for different types of equipment. This could lead to incorrect estimation of FS_L as the exact hammer energy delivered remains unknown. Thus, $(N_1)_{60cs}$ remains ambiguous in such cases.

Based on FC data obtained from particle size classification, the procedure suggested by Boulanger and Idriss [9] has been utilized. The lowest FS_L was estimated at 3 m depth, where FS_L is calculated as 1.1 at 30% ER, and 1.21 at 35% ER, which can be considered potentially liquefiable. If the ER value, which was unmeasured but estimated using previous studies, could have been lower, this layer would show a drop in liquefaction resistance. Figure 33.6 shows FS_L values from SPT-based method for different ER values considered. For comparison with the Indian code provisions, ER = 80% for Donut hammer with trip/auto and ER = 45% for Donut hammer with rope and pulley [13] are also considered in the analysis. 45% ER value gives very high CRR and FS_L at and beyond 7 m (CRR, FS_L approaching infinity). 80% ER leads to very high CRR and FS_L beyond 3 m (CRR = 13.99 and FS_L = 76.31 at 4 m). Hence, those values are not plotted in Fig. 33.6. In general overview, the site seems safe when analysed using SPT-based method as per IS1893 [13] ER assumption. To check how the factor of safety against liquefaction varies when V_S based method is used, further analysis is presented in the next section.

Table 33.1 N-value correction for ER 35%

Depth (m)	N-value	ER %	Energy correction	Rod length correction	$(N_1)_{60}$	FC %	$(N_1)_{60cs}$
1	13	35	0.58	0.75	9.66	24	14.65
2	13	35	0.58	0.75	9.66	32	15.10
3	13	35	0.58	0.75	9.27	32	14.71
4	25	35	0.58	0.85	17.53	26	22.67
5	25	35	0.58	0.85	16.58	26	21.72
6	38	35	0.58	0.95	26.13	8	26.49
7	38	35	0.58	0.95	24.16	8	24.53
8	125	35	0.58	0.95	71.15	25	76.22
10	150	35	0.58	1	87.70	40	93.27
12	107	35	0.58	1	61.47	54	67.08

Fig. 33.6 Factor of safety against liquefaction estimated using N-values for ER values of 30, 35, 40, and 45%



Using V_S profiles

V_S from CHT

V_S profiles from CHT are shown in Fig. 33.2b. The liquefaction analysis results are summarized in Table 33.2. V_S profiles from all the CHT are considered separately, and then the average and minimum V_S values at all depths are considered. It can be observed that based on CHT data, some layers do show a prominent liquefiable tendency contrary to what was observed from the SPT data. Only the layers 1–2 m and 3–4 m have FS_L values close to 1 or ≤ 1 , which can be a concern and need further investigation. For the layers with $V_{S1} > V_{S1}^*$, CRR could not be calculated as these

Table 33.2 Summary of FS_L calculated from CHT data

Depth (m)	CH_32	CH_34	CH_41	CH_45	Average	Minimum
	FS_L	FS_L	FS_L	FS_L	FS_L	FS_L
0–1	1.14	2.27	3.59	0.92	1.51	0.92
1–2	$V_{S1} > V_{S1}^*$	$V_{S1} > V_{S1}^*$	1.74	$V_{S1} > V_{S1}^*$	$V_{S1} > V_{S1}^*$	1.74
2–3	$V_{S1} > V_{S1}^*$	$V_{S1} > V_{S1}^*$	$V_{S1} > V_{S1}^*$	$V_{S1} > V_{S1}^*$	$V_{S1} > V_{S1}^*$	$V_{S1} > V_{S1}^*$
3–4	0.95	10.5	1.11	1.06	1.29	0.95
4–5	3.89	$V_{S1} > V_{S1}^*$	$V_{S1} > V_{S1}^*$	$V_{S1} > V_{S1}^*$	$V_{S1} > V_{S1}^*$	3.89
5–6	$V_{S1} > V_{S1}^*$	$V_{S1} > V_{S1}^*$	$V_{S1} > V_{S1}^*$	$V_{S1} > V_{S1}^*$	$V_{S1} > V_{S1}^*$	$V_{S1} > V_{S1}^*$

Table 33.3 Summary of FS_L calculated from MASW data

Depth (m)	MASW_1	MASW_2	MASW_3	MASW_4	MASW_5	Average	Minimum
	FS_L	FS_L	FS_L	FS_L	FS_L	FS_L	FS_L
0–1	$V_{S1} > V_{S1}^*$	$V_{S1} > V_{S1}^*$	$V_{S1} > V_{S1}^*$	$V_{S1} > V_{S1}^*$	$V_{S1} > V_{S1}^*$	$V_{S1} > V_{S1}^*$	$V_{S1} > V_{S1}^*$
1–2	1.37	1.21	$V_{S1} > V_{S1}^*$	$V_{S1} > V_{S1}^*$	$V_{S1} > V_{S1}^*$	$V_{S1} > V_{S1}^*$	1.21
2–3	0.94	0.83	1.06	1.04	$V_{S1} > V_{S1}^*$	1.32	0.83
3–4	$V_{S1} > V_{S1}^*$	$V_{S1} > V_{S1}^*$	0.82	$V_{S1} > V_{S1}^*$	$V_{S1} > V_{S1}^*$	$V_{S1} > V_{S1}^*$	0.82
4–5	$V_{S1} > V_{S1}^*$	$V_{S1} > V_{S1}^*$	$V_{S1} > V_{S1}^*$	$V_{S1} > V_{S1}^*$	$V_{S1} > V_{S1}^*$	$V_{S1} > V_{S1}^*$	$V_{S1} > V_{S1}^*$
5–6	$V_{S1} > V_{S1}^*$	$V_{S1} > V_{S1}^*$	$V_{S1} > V_{S1}^*$	$V_{S1} > V_{S1}^*$	$V_{S1} > V_{S1}^*$	$V_{S1} > V_{S1}^*$	$V_{S1} > V_{S1}^*$

are not considered liquefiable [7]. FS_L values that can be critical are highlighted in bold.

V_S from MASW

V_S profiles from MASW are shown in Fig. 33.2c. The liquefaction analysis results are summarized in Table 33.3. It can be observed that based on MASW data, some layers do seem to be liquefaction susceptible, much like the CHT data. Layers 2–3 m and 3–4 m have FS_L values close to or ≤ 1 . FS_L values that can be critical are highlighted in bold.

Differences in Results from Different Analyses

The difference in the results from analysis by different methods is quite visible. FS_L obtained from SPT shows higher values than the V_S -based method. To some extent, FS_L from the V_S -based methods does compare well with SPT for 3 m depth when ER is considered as actual without assumption as per IS1893 [13], resulting in a minimum FS_L . Moreover, for depths with V_{S1} exceeding V_{S1}^* , comparison with SPT is not possible. Although the measured ER values help find the layer with the least FS_L , energy measurement should be an integral part of SPT and recommended standard values should not be used blindly, as evident from Fig. 33.6 and already

discussed in the previous section. The FS_L obtained from two V_S -based methods also vary. The primary reason for variation between the two V_S -based calculations is the difference in the V_S profiles. The observed discrepancies between CHT and MASW could be attributed to the picking of the arrival time of the S-wave, as small changes in picked arrival times can lead to significant changes in the estimated V_S . Moreover, water in the borehole casing during the survey may generate tube waves that act as a secondary source of seismic waves inside the borehole. Tube waves are pressure pulses that propagate nearly unattenuated down (and up) the fluid column. These make picking of arrival times difficult.

Conclusion

This study highlights the importance of carrying out multiple geophysical tests to better interpret geotechnical site conditions, which is not possible to obtain using a single type of test. SPT, CHT, and MASW were performed at the same site to determine topographic layers and develop shallow subsurface V_S profile. The two seismic methods delivered different V_S profiles, with CHT giving higher velocities, although the nature of the profiles matched well with the soil profile from borelog, which showed a gradual increase in the stiffness values with depth till the weathered rock layer. N-values and V_S profiles are used to estimate liquefaction resistance using a simplified procedure. The SPT-based method resulted in higher FS_L values in the shallow depth than the V_S -based methods, which showed that the top and subsurface layers at the depth 2–4 m are liquefiable. These differences between different investigation methods are not well understood in the current state of the art and need to be further investigated. This study also highlighted the importance of hammer energy measurement during SPT, as for the same N-value, assuming high ER values (as per IS1893, 2016) would lead to higher FS_L , thus making the results unconservative. It also stresses the need to conduct multiple testing and confirm liquefaction potential to clear the ambiguity introduced because of uncertainty in ER values assumption.

Acknowledgements The authors thank the Dam Safety (Rehabilitation) Directorate, Central Water Commission for funding the project entitled ‘Capacity Buildings in Dam Safety’ under Dam Rehabilitation and Improvement Project. Authors also thank SERB, DST for funding project ‘Development of correction factors for standard penetration test N-values in India through energy measurement and field experiments—Step towards a reliable Liquefaction Potential Assessment’, Ref: SERB/F/198/2017-18 dated 11/05/2017.

References

1. Anbazhagan P, Anjali U, Moustafa SSR, Al-Arifi NSN (2016) Correlation of densities with shear wave velocities and SPT N values. *J Geophys Eng* 13:320–341. <https://doi.org/10.1088/1742-2132/13/3/320>
2. Anbazhagan P, Gajawada P, Moustafa SSR, Al-Arifi NSN, Parihar A (2014) Provisions for geotechnical aspects and soil classification in Indian seismic design code IS-1893. *Disaster Adv* 7(3):72–89
3. Anbazhagan P, Ingale SG (2021) Status quo of standard penetration test in India: a review of field practices and suggestions to incorporate in IS 2131. *Indian Geotech J* 51(2):421–434. <https://doi.org/10.1007/s40098-020-00458-8>
4. Anbazhagan P, Kumar A, Ingle SG, Jha SK, Lenin KR (2021) Shear modulus from SPT N-value with different energy values. *Soil Dyn Earthq Eng* 150:106925. <https://doi.org/10.1016/j.soildyn.2021.106925>
5. Anbazhagan P, Parihar A, Rashmi HN (2012) Review of correlations between SPT N and shear modulus: a new correlation applicable to any region. *Soil Dyn Earthq Eng* 36:52–69
6. Andrus RD, Stokoe KH II (1997) Liquefaction resistance based on shear wave velocity. In: Youd TL, Idriss IM (eds) NCEER workshop on evaluation of liquefaction resistance of soils, Salt Lake City, UT, Technical Report NCEER-97-0022. National Center for Earthquake Engineering Research, Buffalo, NY, pp 89–128
7. Andrus RD, Stokoe KH II (2000) Liquefaction resistance of soils from shear wave velocity. *J Geotech Geoenviron Eng ASCE* 126(11):1015–1025
8. ASTM D4428/D4428M (2014) Standard test methods for crosshole seismic testing. ASTM International, West Conshohocken, PA. www.astm.org
9. Boulanger RW, Idriss IM (2014) CPT and SPT based liquefaction triggering procedures. Report No. UCD/CGM-14/01, Center for Geotechnical Modeling, Department of Civil and Environmental Engineering, University of California, Davis, USA
10. Bowles JE (1996) Foundation analysis and design, 5th edn. The McGraw-Hill Companies Inc., New York
11. Idriss IM (1999) An update of the Seed-Idriss simplified procedure for evaluating liquefaction potential. In: Proceedings of TRB workshop on new approaches to liquefaction analysis, FHWA-RD-99-165, Transportation Research Board, Washington, DC
12. IS 13372-Part 2: Code of practice for seismic testing of rock mass, Part 2: Between the borehole, Bureau of Indian Standards, New Delhi (1992)
13. IS 1893-Part 1: Criteria for Earthquake Resistant Design of Structures, Bureau of Indian Standards, New Delhi, India (2016)
14. Park CB, Miller RD, Xia J (1999) Multichannel analysis of surface waves. *Geophysics* 64(3):800–808
15. Park CB, Miller RD, Xia J (2001) Offset and resolution of dispersion curve in multichannel analysis of surface waves (MASW). In: Proceedings of the SAGEEP 2001, Denver, Colorado, SSM4
16. Seed HB, Tokimatsu K, Harder L, Chung R (1985) Influence of SPT procedures in soil liquefaction resistance evaluations. *J Geotech Eng* 111:1425–1445. [https://doi.org/10.1061/\(ASCE\)0733-9410\(1985\)111:12\(1425\)](https://doi.org/10.1061/(ASCE)0733-9410(1985)111:12(1425))
17. Seed HB, Idriss IM, Arango I (1983) Evaluation of liquefaction potential using field performance data. *J Geotech Eng ASCE* 109(3):458–482
18. Seed HB, Idriss IM (1971) Simplified procedure for evaluating soil liquefaction potential. *J Soil Mech Found Div ASCE* 97(9):1249–1273
19. Sermalai S, Mukundan M, Alagirisamy S (2022) Standard penetration test (SPT) pitfalls and improvements. In: Satyanarayana Reddy CNV, Muthukumaran K, Satyam N, Vaidya R (eds) Ground characterization and foundations. Lecture notes in civil engineering vol 167. Springer, Singapore, pp 363–375. https://doi.org/10.1007/978-981-16-3383-6_33

20. Stokoe KH II, Roesset JM, Bierschwale JG, Aouad M (1988) Liquefaction potential of sands from shear wave velocity. In: Proceedings of 9th world conference on earthquake engineering, Tokyo, Japan, vol III, pp 213–218
21. Verdugo R (2016) Experimental and conceptual evidence about the limitations of shear wave velocity to predict liquefaction. *Soil Dyn Earthq Eng* 91:160–174. <https://doi.org/10.1016/j.soildyn.2016.09.046>
22. Wightman WE, Jalinoos F, Sirles P, Hanna K (2003) Application of geophysical methods to highway related problems. Federal Highway Administration, Central Federal Lands Highway Division, Lakewood, CO, Publication No. FHWA-IF-04-021
23. Xia J, Miller RD, Park CB (1999) Estimation of near-surface shear-wave velocity by inversion of Rayleigh waves. *Geophysics* 64(3):691–700
24. Youd TL, Idriss IM, Andrus RD, Arango I, Castro G, Christian JT, Dobry R, Finn WDL, Harder LF Jr, Koester JP, Liao SSC, Marcuson WF III, Martin GR, Mitchell JK, Moriwaki Y, Power MS, Robertson PK, Seed RB, Stokoe KH II (2001) Liquefaction resistance of soils: summary report from the 1996 NCEER and 1998 NCEER/NSF workshops on evaluation of liquefaction resistance of soils. *J Geotech Geoenviron Eng* 127(10):817–833. [https://doi.org/10.1061/\(asce\)1090-0241\(2001\)127:4\(297\)](https://doi.org/10.1061/(asce)1090-0241(2001)127:4(297))